An Automatic Nuclei Segmentation Technique using Unsharp Masking

Shivam Mishra
ECE PDPM IIITDMJ
Jabalpur, India
21peco11@iiitdmj.ac.in

Amit Vishwakarma
ECE PDPM IIITDMJ
Jabalpur, India
amitv@iiitdmj.ac.in

Anil Kumar
ECE PDPM IIITDMJ
Jabalpur, India
anilkdee@gmail.com

Ronak Vimal
ECE PDPM IIITDMJ
Jabalpur, India
ronakvimal2003@gmail.com

Abstract—Nuclei are very useful in understanding the micro-environment. The pathologist's effort may be reduced and precise micro-environment observations can be obtained by using an automatic nuclei segmentation approach in clinical trials. Even though the latest deep learning (DL) based segmentation algorithms are generally outperforming more conventional approaches, however, this segmentation task is difficult in situations where nuclei are coherent and overlap. In the current study, we propose a novel nuclei segmentation method that combines the U-Net model based on a convolution neural network (CNN) with an unsharp masking technique for the pre-processing of the source images. The unsharp masking technique enhances the high-frequency information of the source images. An objective function is proposed for the optimization algorithm to further improve the segmentation performance. On the same dataset, the efficacy of the suggested method to segment nuclei is compared with existing methods. The suggested technique achieved IOU(JI), Accuracy, Precision, and F1Score values as 0.8172, 96.05%, 0.8672, and 0.8994 respectively. The empirical results reveal that the discussed technique is performing better and is superior to the existing techniques.

Index Terms—Digital image pathology, Nuclei segmentation, U-Net, Unsharp masking

I. INTRODUCTION

Nuclei segmentation is critical work in the evolving field of medical research, with the tremendous potential to accelerate discoveries related to a wide range of diseases, from the most common, such as lung cancer, heart disease, and diabetes, to the rarest. This task is crucial because DNA, the complex genetic code that orchestrates each cell's operations, is found in the nucleus of a cell. We pave the way for a more complete understanding of cellular reactivity to various medications by automating the process of nucleus recognition, giving insights that could possibly change the rate at which solutions for various diseases are produced. This research not only advances the understanding of common conditions such as Alzheimer's and chronic obstructive pulmonary disease, but it also serves as a beacon of hope for mitigating the effects of countless other diseases, transforming countless lives by allowing cures to be realized at an unprecedented rate.

The challenge of segmenting the nuclei in biomedical imaging is particularly due to the nuclei's variability in shape and their overlapping [1]. An overview of a number of digital image pathology methods looking for nuclei in digital images of tissue specimens is given in [2]. Presently, DL-based approaches are widely chosen to perform segmentation tasks due to their promising results. Li *et al*. [3] proposes a semi-supervised Multi-Edge Feature Fusion Attention Network (MEFFA-Net) that uses image, pseudo-mask, and edge features to reduce dependency on labeled samples significantly. The MEFFA-Net improves boundary masks for segmentation by using minimal recognized nuclei borders. The network's MEFFA-Block improves feature selection for accurate segmentation by focusing on nucleus outlines. A novel framework named Kidney-SegNet is introduced by Aatresh *et al*. [4] for image segmentation. This framework combines the efficiency of an attention-based encoder-decoder architecture with the atrous spatial pyramid pooling technique, which uses efficient dimension-wise convolutions. Evaluated on public kidney and TNBC breast H&E stained histopathology image datasets, Kidney-SegNet offered notable advancements in computational complexity and memory requirements, addressing the often overlooked aspects of efficiency in image segmentation models while maintaining high-quality segmentation. A new lightweight PPU-Net model was introduced by Ali *et al*. [5]. The study revealed the efficiency of augmentation and pretraining in circumstances with limited training data, with only 16 images with data augmentation approaching the pixel-wise F1 scores for all models within 5% of those reached with a full dataset. However,

issues such as missed nuclei in dense regions, overlapping cells, and imaging artifacts remained, indicating areas for future development. A deep learning framework discussed by Chanchal *et al.* [6] comprise of high-resolution encoder path, an atrous spatial pyramid pooling bottleneck module, and a powerful decoder. In comparison to benchmark segmentation models with a deep and thin route, this network is wide and deep, using the strength of residual learning as well as encoder-decoder architecture.

Even though DL-based techniques have shown promising results for segmenting nuclei, most of the segmentation algorithms in use today still rely on complex procedures. A new method of preprocessing is being integrated with the U-Net model in order to improve segmentation performance. The main contributions of our suggested method are as follows: a) The unsharp masking technique is used for the pre-processing of source images. This technique is commonly used to highlight details in an image. b) A lightweight U-Net framework is employed for the training and validation of pre-processed dataset images. The U-Net architecture provides the source image's segmented mask. c) The proposed objective function for the optimization algorithm further improves the segmentation performance.

II. MATERIALS AND METHODS

A. Dataset

The dataset was taken from Kaggle [7]. It is difficult to collect data due to the combination of different elements, including cell kind, imaging methods, lighting conditions, etc. The various appearances of the cells can be clearly seen in Fig.1. The illumination condition of the sample is different, which makes it extremely difficult to identify and segment the nuclei. A segmented mask is provided within the dataset for each nucleus shown in the source image. The dataset includes 670 images for the training set, and their segmentation has been recorded as image files. This consists of many imaging modalities, such as CT scans, MRIs, histopathological images, etc.

B. Pre-processing

The unsharp masking technique [8] is used before applying U-Net model to highlight the high-frequency components in an image and thereby increase segmentation performance. Unsharp masking is a digital processing method that is commonly used to highlight details in an image. This is achieved by subtracting a blurred version of
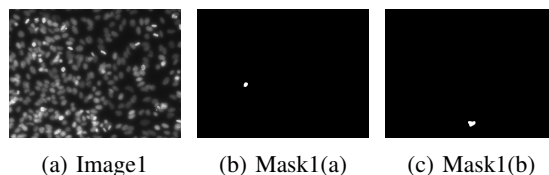

(a) Image1   (b) Mask1(a)   (c) Mask1(b)

Fig. 1: Dataset (source images and masks of two nucleus present in the particular source image)

the image from the original, emphasizing high-frequency components like edges and tiny details. Unsharp masking is given by:

$$EI = OI + (OI{-}BI)XWeight \qquad (1)$$

where EI is the Enhanced Image, OI is the Original Image, and BI is the Blurred Image. The "Weight" specifies how much the high-frequency components are boosted, and the "Blurred Image" is generated with a Gaussian filter with a specified standard deviation. This augmented image is then sent into the U-Net model, which is rich in high-frequency information. With additional input, the model can more rapidly recognize and learn nuanced qualities, allowing for more accurate and refined segmentation.

C. Proposed Technique

Fig.2 displays the flow chart of the suggested technique. In this paper, we offer a novel approach to image segmentation, focused on improving high-frequency information in images to obtain more accurate segmentation. Our suggested solution is divided into three sections: Unsharp Masking for highlighting high-frequency components, U-Net for image segmentation, and proposed objective function for the optimization algorithm. The dataset is initially resized according to the specific dimension of 256 X 256 pixels in our approach. The dataset contains different sizes of images. It's difficult to work with images that vary in size. To perform preprocessing using an unsharp masking technique for source images, subsequent blocks use the resized data as input. The unsharp masking method enhances the high-frequency information of the source images. The U-Net [9] architecture serves as the backbone for our image segmentation task. Because of its effectiveness in identifying complicated structures in images, U-Net is a well-known architecture in biomedical image segmentation. To capture context and localization information, the U-Net idea employs a symmetrical contracting path and an expansive
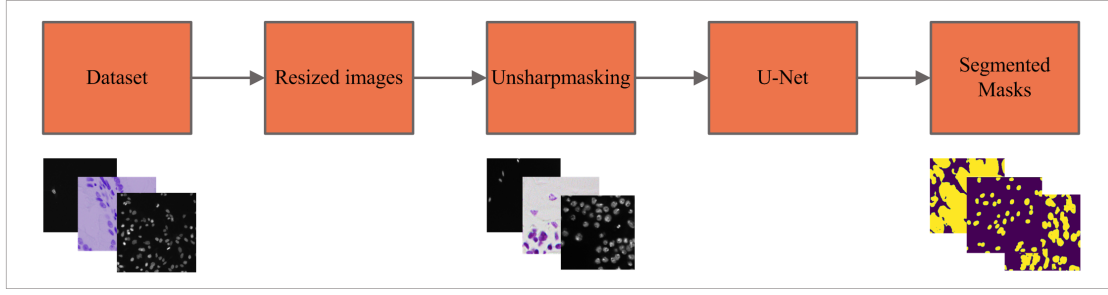
Fig. 2: proposed nuclei segmentation method

path. In the contracting path (encoder), a series of convolutional layers precede a rectified linear unit (ReLU) and a max-pooling layer. This sequential arrangement extracts the hierarchical features of the input images. The expanding path (decoder), on the other hand, is composed of a sequence of up-convolution layers, each followed by a concatenation with the contracting path's proportionally cropped feature map, with the purpose of localizing the high-resolution features. Because the paths are symbiotic, the model can generate fine-grained segmentation maps even with a small number of labeled images. The 2-D convolution operation and Relu are mathematically given by Eqs. (2) and (3), respectively [10].

$$(B \circledast C)(l, m) = \sum_{s,t} B(s,t)C(l+s, m+t) \quad (2)$$

$$Relu(z) = maximum(0, z) \quad (3)$$

The nuclei segmentation performance is further improved by using the proposed objective function. We have used various combinations of Accuracy, Intersection over union (IOU) or Jaccard index (JI), and F1Score metrics as an objective function. The details of these metrics are given in Section III. The optimization algorithm tries to maximize all the metrics in the combination simultaneously and hence, increases the segmentation performance. TABLE I shows the metrics comparisons for various objective functions. On the basis of this comparison, we are proposing the following objective function (OF) for our proposed method:

$$OF = acc. + IOU + F1Score \quad (4)$$

III. EXPERIMENTAL ANALYSIS

This part discusses the results of a number of segmentation techniques that have been applied to an appropriate set of data, together with empirical evidence for the proposed segmentation methodology. The computer used for this study has 16 GB RAM and an Intel(R) Core(TM) i7-3770 CPU. Using multiple metrics, the suggested technique is compared with three standard methods U-Net [9], U-Net++ [11], and U-Net3+ [12]. The performance of the suggested method is analyzed and compared with other approaches using the same dataset. Prior to inserting into the U-Net model, all resized 256 x 256 pixels images were pre-processed using an unsharp masking technique to enhance the high-frequency information of an image. 75% of the source images have been utilized for training, 15% for validation, and 10% for testing. Using the Adam optimizer [13], all networks have been trained. In order to avoid the issue of overfitting or underfitting when applying this method, a dropout value of 0.3 is used. The 25 epochs are completed by all models having a batch size of 16. The performance of the proposed method is evaluated by the intersection over union (IOU) or Jaccard index (JI), accuracy, precision, and F1 score evaluation metrics. This shows the similarity between the two images. These evaluation metrics are given by:

$$IOU(JI) = \frac{tp}{tp + fp + fn} \quad (5)$$

$$Accuracy = \frac{tp + tn}{tp + tn + fp + fn} \quad (6)$$

$$Precision = \frac{tp}{tp + fp} \quad (7)$$

$$F1\,Score = \frac{2tp}{2tp + fp + fn} \quad (8)$$

From Fig.3, it is clear that the suggested technique exceeds the existing techniques in terms of visual quality. The U-Net method's segmentation outputs are displayed in Fig.3 (c, i, o). The figure clearly shows that the output of the U-Net model

(a) Source1   (b) Ground truth   (c) U-NET   (d) U-NET++   (e) U-NET3+   (f) proposed

(g) Source2   (h) Ground truth   (i) U-NET   (j) U-NET++   (k) U-NET3+   (l) proposed
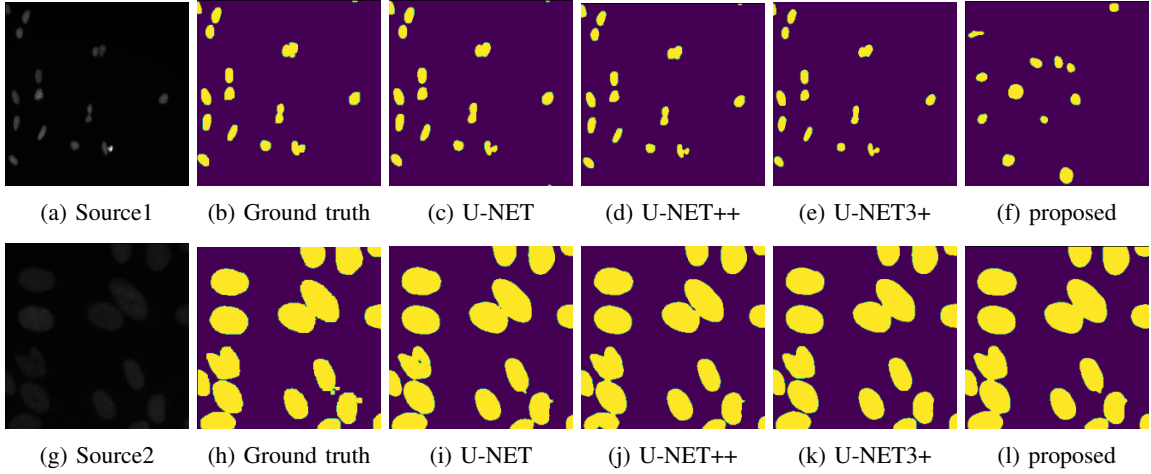
Fig. 3: Qualitative comparison of several segmentation methods

lacks a portion of the ground truth's nuclei. The U-Net framework has an issue of underfitting. Fig.3 (d, j, p) and Fig.3 (e, k, q) show a segmentation result for the UNet++ and UNet3+ models respectively. These models have an overfitting problem. The high-frequency information of the source images is enhanced by using unsharp masking for preprocessing, as shown in Fig.3 (f, l, r), to improve the visual characteristics of the proposed technique. Table II shows the quantitative assessment of this improvement in order to compare the effectiveness of different segmentation techniques. The average IOU(JI) value of the suggested method is 0.8172 and is higher than the average IOU(JI) of U-Net, U-Net++, and U-Net3+ having metric values of 0.7430, 0.7971, and 0.7992 respectively. This assessment metric is frequently used to compare the performance of segmentation. The suggested

method improves its accuracy to 96.05% compared to UNet's, UNet++'s, and UNet3+'s accuracy values of 94.50%, 95.89%, and 95.91%, respectively. Table II shows that the proposed method performs better than either U-Net, U-Net++, and U-Net3+ which have F1Score values of 0.8525, 0.8871, and 0.8879 respectively, with a score of 0.8994. Our proposed technique, on the other hand, has a slightly lower precision value than the existing methods. Results show that our proposed method is more effective than the existing methods for nuclei segmentation. The training and validation accuracy and loss plots for the suggested technique are shown in Fig.4.

IV. CONCLUSION

The most critical step is to have a prompt and correct diagnosis of any illness. A significant method for doing this is the Nuclei segmentation.

TABLE I: Metrics Comparisons of various objective functions

Various objective functions	IOU (JI)	Accuracy	Precision	F1Score
Proposed ($acc.$)	0.8092	95.45%	0.8566	0.8908
Proposed ($acc. + IOU$)	0.8115	95.50%	0.8596	0.8975
Proposed ($acc. + F1Score$)	0.8161	95.43%	0.8670	0.9030
Proposed ($acc. + IOU + F1Score$)	**0.8172**	**96.05%**	**0.8672**	0.8994
Proposed (IOU)	0.8084	95.33%	0.8618	0.8983
Proposed ($F1Score$)	0.8130	95.38%	0.8576	**0.9065**
Proposed ($IOU + F1Score$)	0.8095	95.22%	0.8622	0.8937

TABLE II: Quantitative comparisons of various segmentation models

Methods	IOU (JI)	Accuracy	Precision	F1 score
Ronneberger et al. [9] U-NET	0.7430	94.50%	0.8642	0.8525
Zhou et al. [11] U-NET ++	0.7971	95.89%	0.8857	0.8871
Huang *et al.* [12] U-Net3+	0.7992	95.91%	**0.8863**	0.8879
Proposed ($acc. + IOU + F1Score$)	**0.8172**	**96.05%**	0.8672	**0.8994**

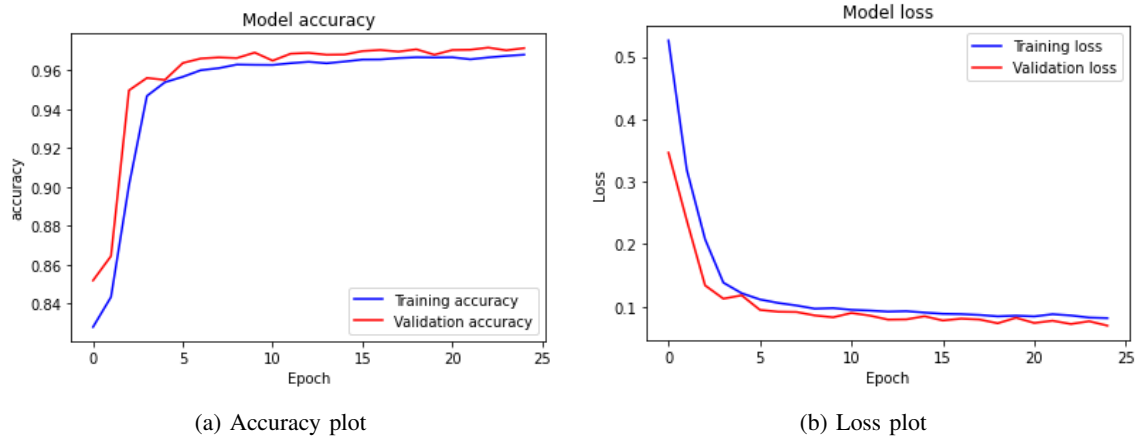(a) Accuracy plot   (b) Loss plot

Fig. 4: Accuracy plot and loss plot of suggested segmentation technique

Disease treatment is dependent on an early diagnosis. The suggested method employs the unsharp masking method for the pre-processing of source images to highlight high-frequency details, allowing us to obtain improved segmentation performance. It takes advantage of the U-Net architecture's strength for initial segmentation. Combining these two approaches makes extracting advanced features from images easier, resulting in more complete and detailed segmentation. The proposed objective function for the optimization algorithm further improves the segmentation results. We compared the proposed method to existing methods both quantitatively and qualitatively. The results prove that the proposed method is capable of performing superiorly to existing methods. However, this proposed method is limited because of the fact that it's not appropriate for instance segmentation. We will try to develop a method that can efficiently perform instance segmentation in the near future.

REFERENCES

[1] S. Mishra, A. Vishwakarma, and A. Kumar, "Automatic nuclei segmentation method using median filter for denoising," in *2023 International Conference on Computer, Electronics Electrical Engineering their Applications (IC2E3)*, 2023, pp. 1–5.

[2] F. Xing, Y. Xie, H. Su, F. Liu, and L. Yang, "Deep learning in microscopy image analysis: A survey," *IEEE transactions on neural networks and learning systems*, vol. 29, no. 10, pp. 4550–4568, 2017.

[3] H. Li, J. Zhong, L. Lin, Y. Chen, and P. Shi, "Semi-supervised nuclei segmentation based on multi-edge features fusion attention network," *Plos one*, vol. 18, no. 5, p. e0286161, 2023.

[4] A. A. Aatresh, R. P. Yatgiri, A. K. Chanchal, A. Kumar, A. Ravi, D. Das, B. Raghavendra, S. Lal, and J. Kini, "Efficient deep learning architecture with dimension-wise pyramid pooling for nuclei segmentation of histopathology images," *Computerized Medical Imaging and Graphics*, vol. 93, p. 101975, 2021.

[5] M. A. Ali, O. Misko, S.-O. Salumaa, M. Papkov, K. Palo, D. Fishman, and L. Parts, "Evaluating very deep convolutional neural networks for nucleus segmentation from brightfield cell microscopy images," *SLAS DISCOVERY: Advancing the Science of Drug Discovery*, vol. 26, no. 9, pp. 1125–1137, 2021.

[6] A. K. Chanchal, S. Lal, and J. Kini, "High-resolution deep transferred asppu-net for nuclei segmentation of histopathology images," *International journal of computer assisted radiology and surgery*, vol. 16, no. 12, pp. 2159–2175, 2021.

[7] "2018 Data Science Bowl — Kaggle." [Online]. Available: https://www.kaggle.com/competitions/data-science-bowl-2018/data

[8] K. N. Shukla, A. Potnis, and P. Dwivedy, "A review on image enhancement techniques," *Int. J. Eng. Appl. Comput. Sci*, vol. 2, no. 07, pp. 232–235, 2017.

[9] O. Ronneberger, P. Fischer, and T. Brox, "U-net: Convolutional networks for biomedical image segmentation," in *International Conference on Medical image computing and computer-assisted intervention*. Springer, 2015, pp. 234–241.

[10] A. Kumar, A. Vishwakarma, and V. Bajaj, "Crccn-net: Automated framework for classification of colorectal tissue using histopathological images," *Biomedical Signal Processing and Control*, vol. 79, p. 104172, 2023.

[11] Z. Zhou, M. M. Rahman Siddiquee, N. Tajbakhsh, and J. Liang, "Unet++: A nested u-net architecture for medical image segmentation," in *Deep Learning in Medical Image Analysis and Multimodal Learning for Clinical Decision Support*. Cham: Springer International Publishing, 2018, pp. 3–11.

[12] H. Huang, L. Lin, R. Tong, H. Hu, Q. Zhang, Y. Iwamoto, X. Han, Y.-W. Chen, and J. Wu, "Unet 3+: A full-scale connected unet for medical image segmentation," in *ICASSP 2020-2020 IEEE international conference on acoustics, speech and signal processing (ICASSP)*. IEEE, 2020, pp. 1055–1059.

[13] Z. Zhang, "Improved adam optimizer for deep neural networks," in *2018 IEEE/ACM 26th international symposium on quality of service (IWQoS)*. Ieee, 2018, pp. 1–2.